

Structural characteristics of chemically synthesized Au nanoparticles

R. Esparza* and G. Rosas

*Instituto de Investigaciones Metalúrgicas, UMSNH,
Edificio U, Ciudad Universitaria, Morelia, Mich. 58000, MEXICO.*

M. López-Fuentes and U. Pal

*Instituto de Física, Universidad Autónoma de Puebla,
Apartado Postal J-48, Puebla, Pue. 72570, MEXICO.*

R. Pérez

*Instituto de Ciencias Físicas, Universidad Nacional Autónoma de México,
P.O. Box 48-3, Cuernavaca, Mor. MEXICO.*

Recibido el 7 de julio de 2006; aceptado el 7 de diciembre de 2006

Metal nanoparticles exhibit unusual chemical and physical properties different from those of the bulk metals, and have a number of fascinating potential applications in heterogeneous catalyst as well as microelectronic and optoelectronic devices. In the present work, a chemical reduction method is used to produce nanometric gold particles. Depending of the concentration of the reducing agent, nanoparticles of different sizes and consequently different atomic structural configurations are obtained. The main structures obtained are fcc-like and decahedral morphologies with fivefold symmetry axes. Using quantum mechanic approximation, the electrophilic fields and the corresponding HOMO-LUMO distributions were calculated.

Keywords: Gold nanoparticles; chemical reduction synthesis; high resolution electron microscopy; structural determination; molecular simulation.

Las nanopartículas metálicas presentan propiedades físicas y químicas diferentes a las de metales en bulto, y tienen varias aplicaciones potenciales en catálisis así como en dispositivos de microelectrónica y optoelectrónica. En el presente trabajo, un método de reducción química es usado para producir partículas nanométricas de oro. Dependiendo de la concentración del agente reductor, se obtienen nanopartículas de diferentes tamaños y consecuentemente diferentes configuraciones estructurales. Las principales estructuras obtenidas son del tipo fcc y decaedrales. Aproximaciones de mecánica cuántica fueron usadas para calcular los campos electrofílicos y las distribuciones de HOMO-LUMO.

Descriptores: Nanopartículas de Au; reducción química; microscopía electrónica de alta resolución; determinación estructural; simulación molecular.

PACS: 61.46.Df; 81.16.Be; 81.07.-b

1. Introduction

The emergence of nanostructured materials has become the subject of novel interest in science and technology since the 1970s. Particles in the nanoregime are of immense importance due to their potential applications in different interdisciplinary fields of physics, chemistry, biology, medicine, and material science. These particles with negligible dimensions exhibit special properties in many aspects compared to those of their bulk counterparts; for example, in catalysis [1-3], in optical properties [4] where the size and shape of the small particles are important, in electronic properties [5,6] and in medical applications [7]. Nanoclusters of metals and semiconductors are of interest because of their size-dependent physicochemical properties originating from the onset of quantum size effects. These nanomaterials are being heralded as the building blocks for designing modern materials [8] for next generation. Gold nanoparticles are among the oldest and best-studied nanoscale materials [9]. They are commercially available in many forms, and numerous synthesis methods for preparing particles from about 1 nm to several micrometers diameter are documented in the literature [10-14]. Nevertheless, only a handful of standard

procedures are employed routinely to prepare gold particles for a multitude of applications. These methods are reliable, simple to carry out, and lead to uniform particles with a narrow size distribution in the desired range. In this work we report the synthesis of Au nanoparticles by a chemical method, which generates clusters in the range of 1–10 nm. The nanoparticles have been characterized by using high-resolution electron microscopy (HREM). The structure determination has been complemented by quantum mechanical calculations based on molecular simulation methods [15].

2. Experimental procedures

The ultra fine gold particles have been obtained using a chemical reduction method [16,17]. Methanol solutions of gold ions were prepared by dissolving crystalline hydrogen tetrachloroaurate ($\text{HAuCl}_4 \cdot x\text{H}_2\text{O}$) in methanol (0.014 mmol in 25 ml of methanol). A methanol solution of PVP [poly (N-vinyl-2-pyrrolidone)] (150 mg of PVP in 25 ml of methanol) was added to the metal ion mixture. To reduce the metal ions, aqueous solutions of NaBH_4 (0.144M) were added drop wise to the PVP containing metal ion mixtures at room temperature (302 K). By adding different amounts of the reducing

solution, the final pH values of the reaction mixtures were adjusted to 3.2, 7.1 and 7.5. Homogeneous colloidal dispersion was formed after the addition of NaBH_4 reductor in the solutions containing the metal ions.

The structural and morphological characteristics of the dispersed metallic nanoparticles have been studied using a Philips Tecnai F20 transmission electron microscope with a field emission gun attachment and dot to dot direct maximum resolution of 0.23 nm. TEM specimens were prepared by dispersing and subsequent drying a drop of colloidal solutions on a copper grid (3 mm in diameter) covered with an amorphous carbon film. The HREM images have been digitally processed.

In order to evaluate the electronic structure and the stability of the nanoparticles, we used quantum mechanical calculations based on the density functional theory (DFT), with a generalized gradient approximation (GGA) for geometry optimizations and for the corresponding electronic based properties (the electrophilic fields and molecular orbital). These calculations were performed using the DMol3 software by Accelrys [18] and considering a Perdew-Wang functional [19]. The configurations of 13 atoms for cubo-octahedral and decahedral structures were studied.

3. Results and discussion

With the purpose of controlling the size and structure of the particles, gold ion solutions of a fixed concentration were reduced with different concentrations of reducing agent (NaBH_4). Fig. 1 shows a series of TEM images obtained for the Au nanoparticles prepared with different contents of the reducing agent (with final pH = 3.2, 7.1 and 7.5). In the sam-

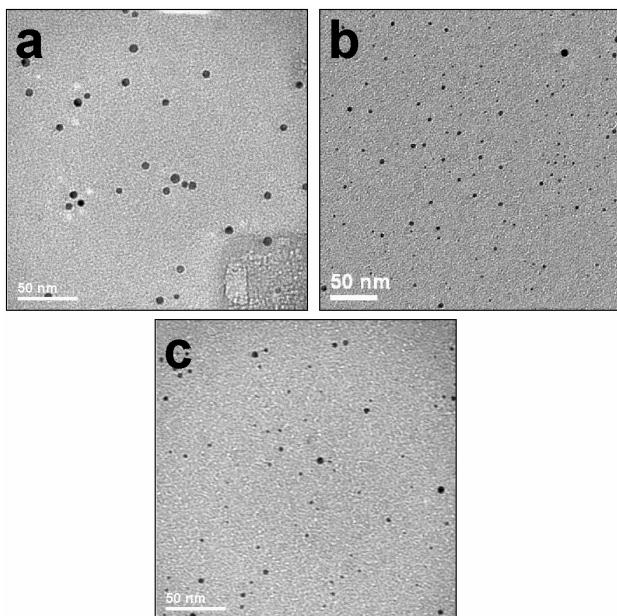


FIGURE 1. Low magnification TEM images of the gold nanoparticles synthesized with different contents of reducing agent, with final pH values a) 3.2, b) 7.1 and c) 7.5 of the reaction mixture.

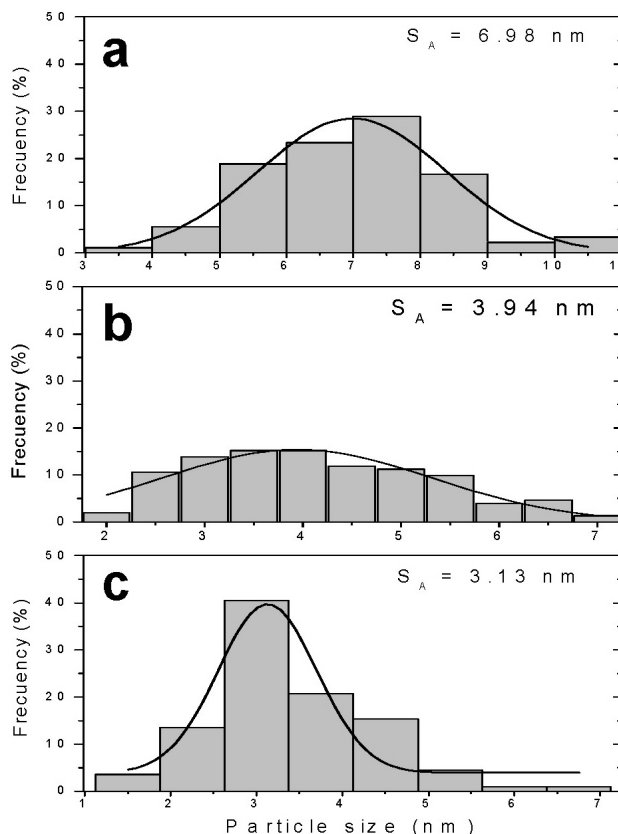


FIGURE 2. Size distribution histograms of the Au nanoparticles prepared at the final pH values a) 3.2, b) 7.1 and c) 7.5 of reaction mixture.

ple with final pH value 3.2 (Fig. 1a), the morphology of the particles is semi-spherical and the formation of agglomerates is not appreciated as reported earlier [20]. The Fig. 1b shows the typical TEM micrograph of the sample prepared with 7.1 final pH value. In this sample, the particles are finer than in the previous case (Fig. 1a). The Fig. 1c shows the typical TEM image corresponding to a 7.5 pH value of the reaction mixture. In this sample, the particles are distributed along the surface and no agglomerates could be appreciated. Although, there are some particles with appreciably large size, the average size of the particles of this sample is smaller and the size distribution is narrower (Fig. 2) in comparison with the previous two samples. Whereas the physical process involving mechanical crushing or pulverization of bulk metals and arc discharge yield large nanoparticles with a wide size distribution, nanoparticles prepared by reduction of metal salts are small with a narrow size distribution.

The Fig. 2 shows the particle size distributions for the samples prepared with different reductor contents. The sample prepared at pH=3.2 (Fig. 2a) produced gold particles in the 5-9 nm size range and of about 6.98 nm average size. When the reducing agent content was adjusted to increase the final pH value to 7.1, for the same concentration of metallic salts (0.014 mmol HAuCl_4), the particle size decreased (Fig. 2b). The average particle size was of about 3.94 nm and

the size of particles varied in the range 2.5 - 5.5 nm. These results suggest that, with the increase of reducing agent content (or the pH value) both the average size and the size dispersion decrease. Figure 2c shows the particle size distribution histogram for the sample prepared at pH=7.5. The average particle size of about 3.13 nm and even narrower size dispersion for this sample supports our previous conclusions. In this sample, up to 40% of the particles were of about 3 nm size. Therefore, for a higher pH value of the reaction mixture, smaller particles of narrow size distribution could be obtained. Physicists predicted that nanoparticles in the diameter range 1-10 nm (intermediate between the size of small molecules and that of bulk metal) would display electronic structures, reflecting the electronic band structure of the nanoparticles, owing to quantum-mechanical rules [21]. The resulting physical properties are neither those of bulk metal nor those of molecular compounds, but they strongly depend on the particle size, inter-particle distance, nature of the protecting organic shell, and shape of the nanoparticles [22]. The intrinsic catalytic activity of the Au nanoparticles was shown to increase with decreasing particle size [23].

The structure of the different Au nanoparticles obtained for different reductor contents was analyzed accurately. For this purpose, HREM images of the samples have been recorded with maximum resolution [24]. Figure 3 shows a series of HREM images for the sample prepared with final pH value of 3.2. In the Fig. 3a, a particle of the STP (single twin particle) type, revealing a twinning joining structure along (111) plane can be observed. The Figs. 3b and 3c show HREM images of two nanoparticles of Au of the fcc-like type, oriented along the [011] and [123] directions, respectively. In the nanoparticle oriented along the [123] direction, there is only a series of fringes where the lattice distance is approximately 2.036 Å, which corresponds to the $d_{200} = 2.039$ Å plane of Au. One of the most stable structures in the nanoparticles of Au besides those of the fcc-like is no doubt, the decahedral [25]. In the Fig. 3d, an HREM image of a decahedral nanoparticle of Au is shown. The FFT clearly shows the characteristic reflections of this type of structure; a group of 10 reflections in a circle indicate that the decahedral particle is oriented along a five-fold axis. This is the only direction which shows this arrangement and it is the most representative of the decahedral structures.

Figure 4 shows a series of HREM images with their respective FFTs for different nanoparticles of Au obtained for final pH = 7.1. The Figs. 4a-4c show three nanoparticles which correspond to decahedrons oriented in the [001] direction or fivefold symmetry axes. It is important to point out that in this sample, a considerable number of decahedrons (60% approximately) were found. According to theoretical data [16], the mtp (multiple twin particles) type nanoparticles are catalytically more active than the fcc-like nanoparticles. Therefore, we assume that this sample might have better catalytic properties in comparison with the other samples prepared with the same concentration of metallic salts (0.014 mmol of HAuCl_4 in 50 ml of total reaction mixture). On the

other hand, the Fig. 4d shows a nanoparticle of the fcc-like type oriented along the [123] direction. This type of structure was found in approximately 40% of the observed nanoparticles.

The morphology of the Au nanoparticles depends strongly on the metal ion concentration and the reducing

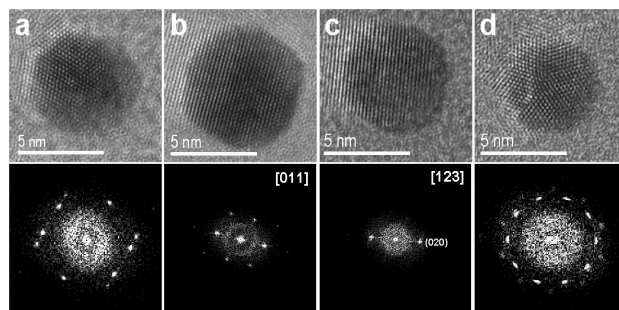


FIGURE 3. HREM images of gold nanoparticles with their respective power spectra prepared with pH=3.2 of the reaction mixture. a) Single twinned particle, b) and c) fcc-like particles, and d) decahedron particle.

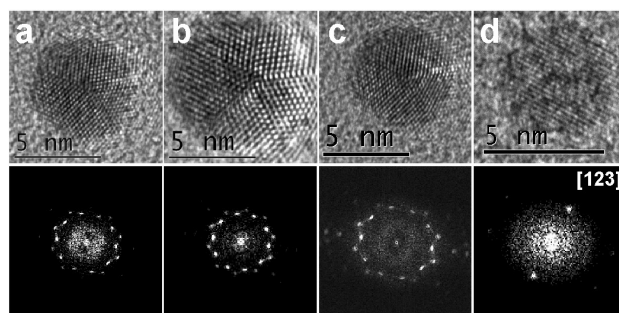


FIGURE 4. HREM images of gold nanoparticles with their respective power spectra. The sample was prepared with pH=7.1 of reaction mixture. a), b) and c) decahedron particles, and d) fcc-like particle.

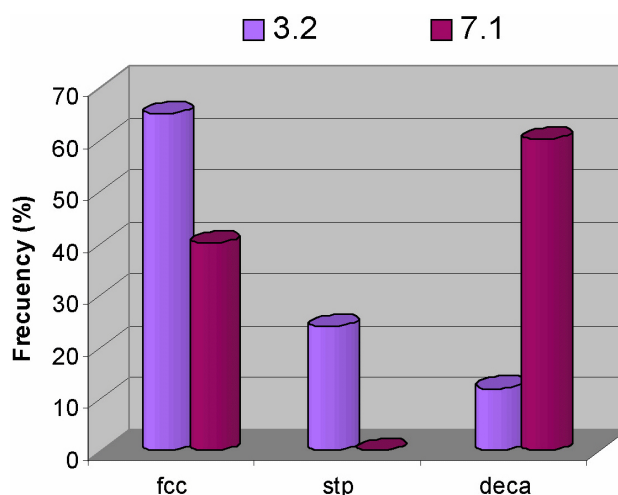


FIGURE 5. Frequency of the structural morphologies of the different nanoparticles as a function of final pH of the reaction mixture.

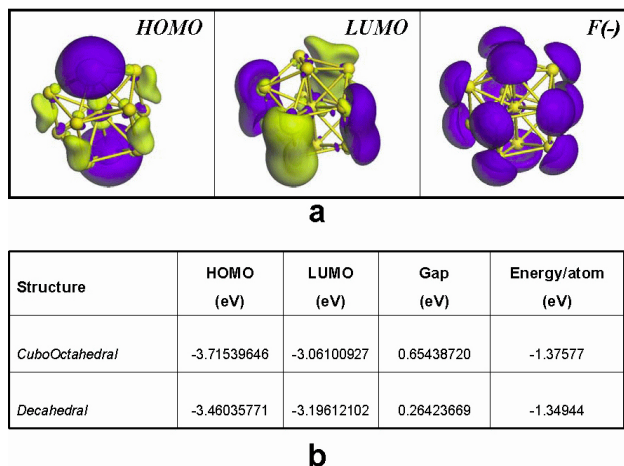


FIGURE 6. a) HOMO, LUMO and the electrophilic field for the decahedral Au₁₃ structure and b) the comparison of values between cubo-octahedral and decahedral configurations.

agent content in the reaction mixture. When solution of a fixed metal ion concentration (0.014 mmol of HAuCl₄ in 50 ml total of reaction mixture) was reduced with two different amounts of the reducing agent (final pH=3.2 and 7.1), the morphologies of the particles are totally different. This is illustrated in the Fig. 5. For the sample prepared at pH=3.2, the main structures were: fcc-like type (64%), a smaller quantity of the single twin particle (24%) and, finally about 12% of decahedral structures. On the other hand, the Au sample prepared with pH= 7.1, contrary to the previous sample, the main structures were of the decahedral type (60%) with a smaller percentage of the fcc-like type structures (40%).

As a first insight on the stability of nanoparticles with different structures, the conditions of stability and electronic properties of decahedron and cubo-octahedron configurations have been studied. In Fig. 6a both molecular orbital and the electrophilic field iso-surface distributions for a decahedron Au₁₃ are shown. The differences become really evident in both types of molecular orbitals. For the HOMO, charge is distributed mainly at the outer surface of the cluster, and for the LUMO, it is localized mainly in the body or central region of the cluster, while the electrophilic field clearly shows that the body has a homogeneous negative charge distribution.

The introduction of electronegativity as a DFT reactivity descriptor can be traced back to the consideration of the

response of a system (atom, molecule, etc.) when it is perturbed by a change in its number of electrons at a fixed external potential. The resulting quantities (electronegativity) correspond to the response of the energy of the system to electrophilic perturbations. Since the Fukui functions represent a variation of the chemical potential induced by an external perturbation. When this variation is high, the system would be more reactive. The points or positions with higher electronegativity values are more reactive to the external perturbation. In the case of decahedral structure, the electrophilic field is located around the whole cluster. Therefore, it is assumed that this structure has a higher reactivity in comparison with the fcc-like structure [20].

A comparison between the HOMO-LUMO gap and the energy per atom values for decahedron and cubo-octahedron configurations (Fig. 6b) allows understanding that the decahedron is a better conductor. However, both are stable configurations and the presence of them in our samples must increase the catalytic applications of the material.

4. Conclusions

The used synthesis method allows preparing gold particles of the nanometric (1-10 nm) size range in a controlled manner. Both the average particle size and the size dispersion are small when the amount of reducing agent in the reduction reaction is high or in other words, the pH of the reaction mixture is high. The fcc-like structure, which is the main and common structural type of gold nanoparticles, is obtained when the pH of the reaction mixture is acidic (3.2). Higher pH value of the reaction mixture generates mainly decahedral type structures. Our quantum mechanical theoretical analysis reveals that the decahedral structures are catalytically more active and better conductors (electrical) than the structures of the fcc-like type.

Acknowledgment

We would like to acknowledge the technical support of A. Medina in taking the High-Resolution Electron Microscopic images of the samples.

* Corresponding author; e-mail: roesparza@gmail.com, Phone: +52 (443) 322 3500 Ext. 4032, Fax: +52 (443) 322 3500 Ext. 4010

1. N. Lopez *et al.*, *Journal of Catalysis* **223** (2004) 232.
2. M. Haruta, *Journal of New Materials for Electrochemical Systems* **7** (2004) 163.
3. Radha Narayanan and Mostafa A. El-Sayed, *J. Phys. Chem. B* **109** (2005) 12663.

4. Yong Lei and Wai-Kin Chim, *J. Am. Chem. Soc.* **127** (2005) 1487.
5. B.L. Cushing *et al.*, *Nanotechnology* **16** (2005) 1701.
6. L.R. Hirsch *et al.*, *Proc. Natl. Acad. Sci. USA* **100** (2003) 13549.
7. Randolph Fillmore, *Nanomedicine: Nanotechnology, Biology, and Medicine* **2** (2006) 49.
8. Bharat Bhushan Ed., *MEMS/NEMS Devices and Applications*

- (Topics in Handbook of Nanotechnology, Springer-Verlag, Berlin 2004) p. 225.
9. M.C. Daniel and D. Astruc, *Chem. Rev.* **104** (2004) 293.
 10. J. Wagner and J.M. Köhler, *Nano Letters* **5** (2005) 685.
 11. Y.F. Guan and A.J. Pedraza, *Nanotechnology* **16** (2005) 1612.
 12. R. Harpeness and A. Gedanken, *Langmuir* **20** (2004) 3431.
 13. Chun-Hong Kuo and Michael H. Huang, *Langmuir* **21** (2005) 2012.
 14. I. Hussain, M. Brust, A.J. Papworth, and A.I. Cooper, *Langmuir* **19** (2003) 4831.
 15. B. Gilbert, F. Huang, H. Zhang, G.A. Waychunas, and J.F. Banfield, *Science* **305** (2004) 651.
 16. R. Esparza *et al.*, *J. Nanosci. Nanotechnol.* **5** (2005) 641.
 17. U. Pal, J.F. Sanchez, S.A. Gamboa, P.J. Sebastián, and R. Pérez, *Phys. Stat. Solid. C* **8** (2003) 2944.
 18. B. Delley, *J. Chem. Phys.* **113** (2000) 7756.
 19. J.P. Perdew and Y. Wang, *Phys. Rev. B* **45** (1992) 13244.
 20. R. Esparza *et al.*, *Mater. Charac.* (On line).
 21. A.P. Alivisatos, *Science* **271** (1996) 933.
 22. M. Brust and C.J. Kiely, *Colloids Surf. A: Physicochem. Eng. Asp.* **202** (2002) 175.
 23. L. Guzzi, D. Horváth, Z. Pászti, and G. Pető, *Catal. Today* **72** (2002) 101.
 24. M. José Yacamán, J.A. Ascencio, S. Tehuacanero, and M. Marín, *Topics in Catalysis* **18** (2002) 167.
 25. J.A. Ascencio, M. Pérez-Alvarez, S. Tehuacanero, and M. José-Yacamán, *Appl. Phys. A* **73** (2001) 295.